Noname manuscript No.
(will be inserted by the editor)

Regularized Model of Post-Touchdown Configurations in Electrostatic MEMS: Bistability Analysis.

A. E. Lindsay

Received: July 28, 2015

Abstract This paper considers the problem of stiction in electrostatic-elastic deflections whereby elastic surfaces adhere to one another after coming into physical contact under attracting Coulomb interactions. This phenomenon is studied in a family of recently derived models which account for forces which become important when the elastic surfaces are in close proximity. The presence of bistability in these models results in hysteresis, or non reversibility, which accounts for the difficulty in achieving separation after an initial contact event. We use singular perturbation techniques to derive explicit formula for the critical parameters over which bistability occurs and discuss new operational modes which arise when bistability is present.

Keywords Singular perturbation techniques · nano-technology · stiction · Van der Waals forces · Casimir forces · higher order partial differential equations.

1 Introduction

Micro electromechanical Systems (MEMS) combine moving elastic component with electrostatic forces on miniature scales to perform a variety of tasks in engineering applications. When the attracting electrostatic forces are large enough, the elastic components of the device may come into physical contact - an event known as *touchdown* or *snap-through*. This outcome may be undesirable or essential in normal operation, depending on the particular application. In either scenario, it is desirable that the device is able to revert to a base state after touchdown. However, after initial contact, the elastic surfaces may adhere to one another thus complicating the return to a separated state. This phenomenon, also known as *stiction*, is due to Casimir, capillary and Van der Waals forces which become prominent on very small separation scales and is a major problem in the fabrication and operation of MEMS (cf. [1–3]).

Canonical mathematical models (cf. [4–7]) of MEMS do not shed light on the problem of stiction as they capture contact events as finite time singularities of the governing equations, thus providing no information on subsequent configurations of the device. A recently introduced model (cf. [8]) is a first attempt to mathematically investigate these post-touchdown states by including a thin insulating layer which prevents physical contact between the deflecting surface and the substrate (cf. Fig. 1). These models are partial differential equations whose solutions represent the deflection of an elastic

A. E. Lindsay
Department of Applied and Computational Mathematics and Statistics
University of Notre Dame,
South Bend, Indiana, 46556, USA.
E-mail: a.lindsay@nd.edu

surface under Coulomb forcing. If the deflecting surface is represented as a one-dimensional flexible elastic beam on $\Omega = [-1, 1]$, then the non-dimensional deflection $u(x, t)$ was shown (cf. [8]) to satisfy the fourth order partial differential equation

$$u_t = -u_{xxxx} - \frac{\lambda}{(1+u)^2} + \frac{\lambda\varepsilon^{m-2}}{(1+u)^m}, \quad x \in (-1, 1); \qquad u(\pm 1) = u_x(\pm 1) = 0, \tag{1.1}$$

where $\lambda \geq 0$ is a bifurcation parameter which depends on the voltage applied to the system. In terms of physical quantities, the two dimensionless parameters in (1.1) are given by (cf. [8])

$$\lambda = \frac{\varepsilon_0 L^4 V^2}{2dEI}, \qquad \varepsilon = \frac{d\sigma_0}{h\sigma_1},$$

where L, d and h are the characteristic length scales of the device, the gap spacing and the insulating layer (cf. Fig. 1). The parameter ε is determined in terms the geometrical ratio d/h and the ratio σ_0/σ_1 of dielectric constants in the insulating layer and the gap. The parameter V is the potential difference between the deflecting surface and the substrate, ε_0 is the permittivity of free space and EI is the flexural rigidity of the deflecting plate. The present work focuses on understanding the bifurcation structure, and in particular the bi-stable properties, of one dimensional equilibrium solutions to (1.1).

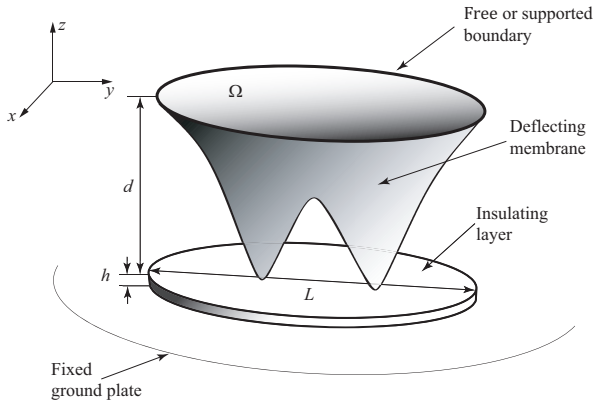

Fig. 1 Schematic diagram of the regularized MEMS device. Reproduced from [8].

The regularizing term $\varepsilon^{m-2}(1+u)^{-m}$ for $m > 2$ can account for a variety of physical effects which come into play when $u \approx -1$ and play a role in stiction. For example $m = 4$ accounts for the Casimir force, a quantum effect which manifests itself on macroscopic scales [9, 10]. The case $m = 3$ models Van der Waals forces [9, 11, 12]. The particular force that dominates when the spacing is small depends on the particular geometry of the device and application. Casimir forces scale as $F_{Cas} \propto d^{-4}$ while Van der Waals forces scale like $F_{VdW} \propto d^{-3}$ where d is the dimensional gap spacing (cf. Fig. 1). In certain scenarios, both forces may be of equal importance and the inclusion of two regularizing terms would be justified [3, 13]. Regularizing potentials of this form have also been extensively utilized in studies of the de-wetting process of thin films on solid substrates [14–17].

In canonical models of MEMS for which $\varepsilon = 0$, touchdown occurs when λ exceeds a threshold λ^* and $u \to -1$ in a finite time T. Since this event is crucial to the operation of MEMS, many studies have focussed on analyzing the local structure of solutions to (1.1) in this regime and estimation of parameters T and λ^* (cf. [4, 6, 7, 18, 19]). However, the manifestation of touchdown as a singularity of (1.1) is a serious limitation of the canonical model as no information is provided regarding subsequent configurations of the system.

The regularized model (1.1) with suitable initial data is globally well posed for $\varepsilon > 0$ [8]. This key property follows because (1.1) arises from the L^2 gradient flow of the energy functional

$$\mathcal{E}(u) = \int_0^1 \left(\frac{1}{2}|u_{xx}|^2 - \frac{\lambda}{(1+u)} + \frac{\lambda\varepsilon^{m-2}}{(m-1)(1+u)^{m-1}} \right) \mathrm{d}x.$$

which is dissipative ($d\mathcal{E}/dt \leq 0$) and bounded from below. The possibilities for the limiting behavior of dynamic solutions to (1.1) as $t \to \infty$ are therefore related to the multiplicity and stability of solutions to the steady state problem

$$-u_{xxxx} = \frac{\lambda}{(1+u)^2} - \frac{\lambda\varepsilon^{m-2}}{(1+u)^m}, \quad x \in (-1,1); \qquad u(\pm 1) = u_x(\pm 1) = 0. \tag{1.2}$$

In the present work, the focus is on studying solution multiplicity of (1.2) as the parameters ε and m vary.

The numerically obtained bifurcation diagrams of (1.2), displayed in Fig. 2, show that there are two remarkable departures from the $\varepsilon = 0$ case. First, there is a new maximal solution branch representing post-touchdown (contact) steady states. This branch of equilibria is characterized (cf. [8] for derivation and validation) by the following asymptotic parameterization in terms its squared L^2 norm

$$\|u(x;\varepsilon)\|_2^2 = 2\left[1 - \frac{22}{35}\left(\frac{18\varepsilon(m-1)}{\lambda(m-2)}\right)^{\frac{1}{4}} + \mathcal{O}(\varepsilon^{\frac{3}{4}})\right], \tag{1.3}$$

in the limit as $\varepsilon \to 0$. Second, it is clear that the multiplicity of equilibrium solutions to (1.2) can be quite different depending on the value of the parameter ε. More precisely, the bifurcation diagrams suggest the existence of a critical value ε_c such that for $\varepsilon \geq \varepsilon_c$, equation (1.2) has a unique solution for each λ. In the case where $0 < \varepsilon < \varepsilon_c$, the bifurcation diagrams have two saddle node bifurcation points $\lambda_*(\varepsilon)$ and $\lambda^*(\varepsilon)$. Correspondingly, for $\lambda_* < \lambda < \lambda^*$, equation (1.2) admits three solutions, while for $\lambda > \lambda^*$ and $\lambda < \lambda_*$, there is a unique solution.

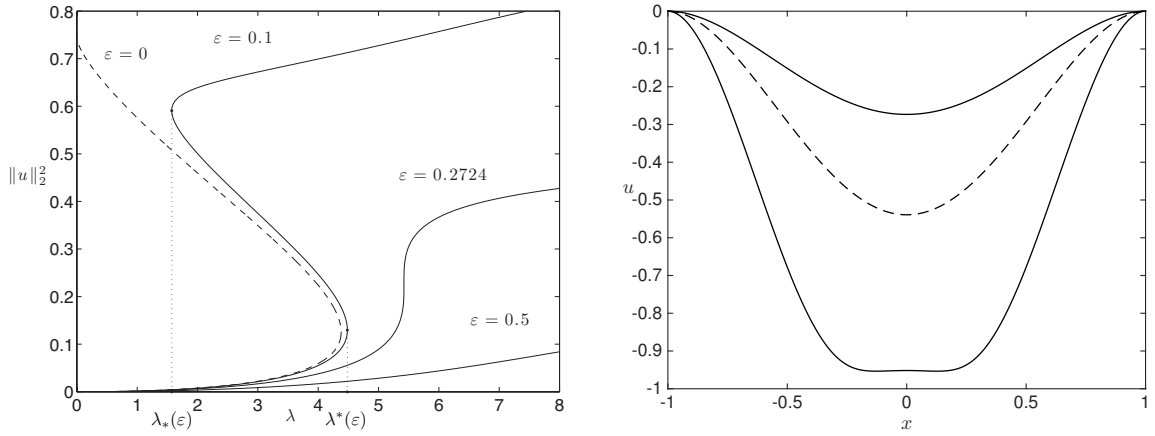

(a) Bifurcation curves of (1.2).

(b) Stable (solid line) and unstable (dashed line) profiles for $\lambda = 4$ and $\varepsilon = 0.05$.

Fig. 2 Left Panel: Bifurcation curves for equilibrium solutions of (1.2) for $m = 4$. The three solid curves plotted correspond to $\varepsilon < \varepsilon_c$, $\varepsilon \approx \varepsilon_c$ and $\varepsilon > \varepsilon_c$ highlight the threshold of bistability. The dashed curve is the solution set associated with the $\varepsilon = 0$ problem. Right Panel: Stable (solid lines) and unstable (dashed line) solution profiles of (1.2) for $\lambda = 4$ and $\varepsilon = 0.05$. The upper profile represents a separated state, while the lower profile represents a contact state of the device. Multiple minima in the contacted state arise from a non-monotone boundary layer profile in the vicinity of the contact points (cf. [8]).

The potential for bistability over the range of values $0 < \varepsilon < \varepsilon_c$ has several practical implications for the construction of MEMS (cf. [20–22]). Robust switching behavior can be generated from bistable systems, specifically the system can transition between stable large and small norm solutions over the parameter window $\lambda \in (\lambda_*(\varepsilon), \lambda^*(\varepsilon))$. Additionally, Fig. 2 also reveals the presence of hysteresis, or non-reversibility, in (1.1) for $\varepsilon < \varepsilon_c$ and therefore captures the stiction phenomenon. For $\lambda > \lambda^*$, the

device is in a stable state with surfaces in contact. To unstick the device however, λ must be decreased below the second fold point λ_* where $\lambda_* < \lambda^*$. For a detailed study of the transient dynamics between stable states of (1.1), see [23].

The important practical problem addressed in this work is the quantification of the key thresholds ε_c, $\lambda^*(\varepsilon)$ and $\lambda_*(\varepsilon)$ in (1.2) for $m > 2$. The approach undertaken is a detailed asymptotic analysis of equations (1.2) in the limit as $\varepsilon \to 0^+$, the result of which is explicit formulas for the fold points $\lambda^*(\varepsilon)$ and $\lambda_*(\varepsilon)$ for $m > 2$. A heuristic approximation of the critical parameter ε_c can then be obtained from the condition

$$\lambda^*(\varepsilon_c) = \lambda_*(\varepsilon_c). \tag{1.4}$$

In engineering studies of MEMS, mathematical models typically feature fourth order terms such as (1.2) as these descriptions give good quantitative agreement with experiments. On the other hand, mathematical studies of MEMS are largely focussed on second order equations which describe the deflecting surface as a tensioned membrane and rely on maximum principles for their analysis. The present work is focussed solely on the fourth order model for two main reasons. First, the explicit formulas developed in the present work are useful to MEMS practitioners who seek to exploit bistability in the operation of these devices. Second, while the Laplacian counterpart of (1.2) (with $\partial_n u|_{\partial\Omega} = 0$ omitted) also exhibits the bistability structure observed in Fig. 2, its analysis is better suited to a phase plane approach (cf. Sec. 3.4 of [8]). A dynamical systems approach does not naturally extend to the fourth order problem and so we adopt a singular perturbation analysis of (1.2) as $\varepsilon \to 0$. For recent mathematical studies on the existence of solutions to the second order counterpart of (1.1) in the case $m = 4$, see [24, 25].

The structure of the paper is as follows. In Sec. 2, the dependence of the principal fold point λ^* of (1.2) on ε and m is analyzed in the limit as $\varepsilon \to 0$. Through a regular perturbation analysis, the formula

$$\lambda^*(\varepsilon) = \lambda_0 + \varepsilon^{2(m-2)}\lambda_1 + \mathcal{O}(\varepsilon^{4(m-2)}),$$

is established in Principal Result 1 and values of λ_0 and λ_1 calculated for a range of m.

In Sec. 3, we calculate the secondary saddle node bifurcation point $\lambda_*(\varepsilon)$ in the limit $\lambda_*(\varepsilon) \to 0$ as $\varepsilon \to 0$. This fold point is not present in the case $\varepsilon = 0$ and its location requires a detailed singular perturbation calculation with systematic use of logarithmic switchback terms. These terms are well known in the asymptotic analysis of high Reynold's number flow problems [26–29] and in other singular perturbation problems related to MEMS [19, 30]. In Principal Result 2, we obtain the expansion

$$\lambda_*(\varepsilon) \sim \varepsilon^{\frac{3}{2}}\lambda_0 + \varepsilon^2\lambda_1 + \cdots$$

where λ_0 and λ_1 are determined in terms of m. Combining Principal Results 1 and 2 gives an asymptotic prediction (cf. (3.29)) for the bistable parameter range $\lambda_* < \lambda < \lambda^*$ of equation (1.2). For example, in the case $m = 4$, we find that range to be

$$61.4586\,\varepsilon^{\frac{3}{2}} - 41.8124\,\varepsilon^2 < \lambda < 4.3809 + 9.9713\,\varepsilon^2. \tag{1.5}$$

By numerically solving for the value of ε at which this bistable range shrinks to a point, an estimate can be formulated for the critical ε_c (cf. Sec. 3.1 and Principal Result 3). In the case $m = 4$ for example, we obtain an asymptotic estimate of $\varepsilon_c \approx 0.2468$ which compares well ($\approx 10\%$) with the numerical estimate $\varepsilon_c \approx 0.2724$. In Sec. 4 we discuss avenues for future investigation.

2 Asymptotics of the fold point of the minimal branch

In this section, we calculate the effect of the perturbed potential on the location of the fold point $\lambda^*(\varepsilon)$, located at the end of the minimal solution branch of the equilibrium problem (1.2). The solution set $(\lambda(\varepsilon), u(x;\varepsilon))$ of (1.2) can be computed numerically by first specifying the squared L^2 norm of

solutions, then formulating the MATLAB boundary value problem solver `bvp4c` to obtain λ as a constant parameter.

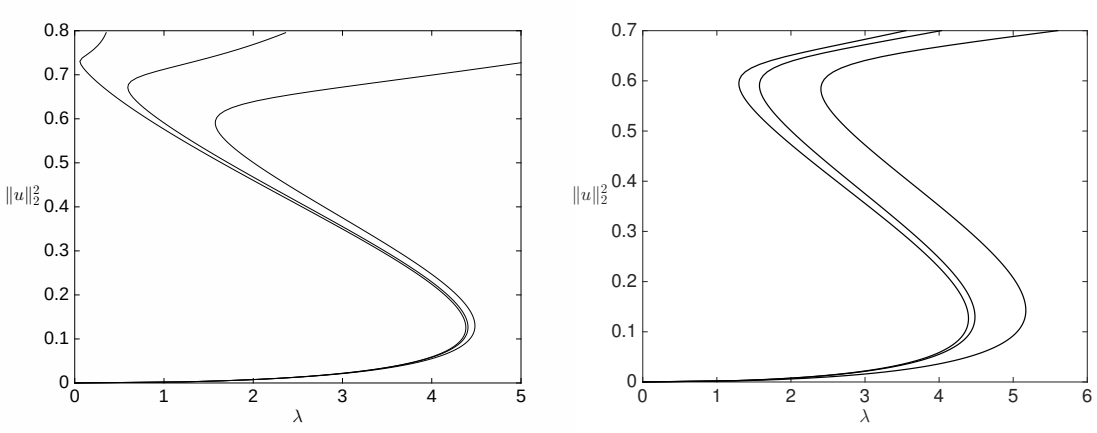

(a) Fixed $m = 4$. (b) Fixed $\varepsilon = 0.1$.

Fig. 3 Bifurcation diagrams of equilibrium solutions of (1.2). Left panel, $m = 4$ and $\varepsilon = 0.1$, 0.05, 0.01. Right panel: $\varepsilon = 0.1$ and $m = 3$, 4, 5.

The fold point $\lambda^*(\varepsilon)$ is calculated by means of a regular expansion of (1.2), developed in the limit as $\varepsilon \to 0$. See also [31–33] for more background on this approach. This approach will not work for the secondary saddle-node bifurcation $\lambda_*(\varepsilon)$ which is not present in the $\varepsilon = 0$ case. This second threshold indicates the onset of the large norm solution branch and is located at the end of the unstable branch of equilibria emanating from the first saddle-node.

Let us assume a parameterization of the minimal solution branch in terms of the squared L^2 norm $\alpha = \|u(x;\varepsilon)\|_2^2$, of equilibrium solutions. A two term expansion of the solution, valid for u away from -1, is given by

$$u = u_0(x;\alpha) + \varepsilon^{m-2}u_1(x;\alpha) + \mathcal{O}(\varepsilon^{2(m-2)}), \qquad \lambda = \lambda_0(\alpha) + \varepsilon^{m-2}\lambda_1(\alpha) + \mathcal{O}(\varepsilon^{2(m-2)}). \tag{2.1}$$

The location of the principal fold point is expanded in a regular fashion as

$$\alpha^*(\varepsilon) = \alpha_0^* + \varepsilon^{m-2}\alpha_1^* + \cdots$$

where the α_j are determined by the condition that $d\lambda/d\alpha = 0$ independent of ε. The principal fold (λ^*, α^*), then admits the two term expansion

$$\lambda^*(\varepsilon) = \lambda(\alpha^*) = \lambda_0(\alpha_0^*) + \varepsilon^{m-2}\lambda_1(\alpha_0^*) + \mathcal{O}(\varepsilon^{2(m-2)}). \tag{2.2}$$

To complete the two term expansion (2.2), the quantity $\lambda_1(\alpha_0^*)$ is now determined by applying the expansion (2.1) to equation (1.2) and arriving at the problems

$$-u_{0xxxx} = \frac{\lambda_0}{(1+u_0)^2}, \quad -1 < x < 1; \qquad u_0(\pm 1) = u_{0x}(\pm 1) = 0. \tag{2.3a}$$

$$\mathcal{L}u_1 = \frac{\lambda_1}{(1+u_0)^2} - \frac{\lambda_0}{(1+u_0)^m}, \quad -1 < x < 1; \qquad u_1(\pm 1) = u_{1x}(\pm 1) = 0. \tag{2.3b}$$

where $\mathcal{L}$ is the linearized operator

$$\mathcal{L}\phi = -\phi_{xxxx} + \frac{2\lambda_0}{(1+u_0)^3}\phi.$$

m	3	4	5	6	7	8
$\lambda_1(\alpha_0^*)$	6.5715	9.9690	15.2703	23.5847	36.6840	57.4034

Table 1 Numerical values of correction term $\lambda_1(\alpha_0^*)$ in the asymptotic expansion of the saddle-node fold point (λ^*, α^*) for $m = 3, 4, \ldots, 8$.

The location of the principal fold point of (2.3a) is $(\alpha_0^*, \lambda_0(\alpha_0^*))$ and satisfies $\lambda_{0\alpha}(\alpha_0^*) = 0$. The coordinates of this principal fold point can be accurately located by Newton-Raphson iterations and has the numerical value

$$(\alpha_0^*, \lambda_0(\alpha_0^*)) = (0.1256, 4.3809). \tag{2.4}$$

To calculate the quantity $\lambda_1(\alpha_0^*)$, equation (2.3b) is differentiated with respect to α to reveal that at $\alpha = \alpha_0^*$, $\lambda_{0\alpha} = 0$ and consequently there is a nontrivial solution satisfying $\mathcal{L}u_{0\alpha} = 0$. This provides a solvability condition of (2.3b) at $\alpha = \alpha_0^*$ which fixes the correction term

$$\lambda_1(\alpha_0^*) = \lambda_0(\alpha_0^*)\frac{\displaystyle\int_{-1}^{1} \frac{u_{0\alpha}}{(1+u_0)^m}\,\mathrm{d}x\Big|_{\alpha=\alpha_0^*}}{\displaystyle\int_{-1}^{1} \frac{u_{0\alpha}}{(1+u_0)^2}\,\mathrm{d}x\Big|_{\alpha=\alpha_0^*}} = \lambda_0(\alpha_0)\frac{I_1}{I_2} \tag{2.5}$$

in terms of the two integrals I_1 and I_2 give rise to the two term expansion. These integrals are easily evaluated numerical by first noticing that

$$I_1 = -\frac{\partial}{\partial\alpha}\Big[\int_{-1}^{1} \frac{\mathrm{d}x}{(m-1)(1+u_0)^{m-1}}\Big]_{\alpha=\alpha_0^*}, \qquad I_2 = -\frac{\partial}{\partial\alpha}\Big[\int_{-1}^{1} \frac{\mathrm{d}x}{(1+u_0)}\Big]_{\alpha=\alpha_0^*}.$$

The values of the correction $\lambda_1(\alpha_0^*)$ are given in Table. 1 for several m.

Principal Result 1 *In the limit as $\varepsilon \to 0$, the principal fold points λ^* of the equilibrium problems* (1.2) *admits the two term expansion*

$$\lambda^*(\varepsilon) = \lambda_0(\alpha_0^*) + \varepsilon^{m-2}\lambda_1(\alpha_0^*) + \mathcal{O}(\varepsilon^{2(m-2)}), \tag{2.6}$$

where $(\lambda_0(\alpha_0^*), \alpha_0^*)$ and $\lambda_1(\alpha_0^*)$ represent the principal fold point of the unperturbed problem and its correction respectively. The numerical value of $(\lambda_0(\alpha_0^*), \alpha_0^*)$ is given in (2.4) *while $\lambda_1(\alpha_0^*)$ is given by* (2.5)*.*

As an example of Principal Result 1 in the case $m = 4$, the fold point λ^* has the expansion

$$\begin{aligned} \lambda^* &= \lambda_0(\alpha_0^*) + \lambda_1(\alpha_0^*)\,\varepsilon^2 + \mathcal{O}(\varepsilon^4) \\ &= 4.3809 + 9.9690\,\varepsilon^2 + \mathcal{O}(\varepsilon^4). \end{aligned} \tag{2.7}$$

In Fig. 4, the agreement between the expansion (2.7) and the full numerical calculation of the fold point is plotted.

3 Asymptotics of the secondary fold point

In this section, we construct the solutions to the steady state deflection problem (1.2) in the vicinity of the second saddle node bifurcation point λ_*. This second fold point is located at the end of the unstable branch emanating from the principal fold point. In contrast to the regular expansions developed in section Sec. 2, a singular perturbation will be required as the fold point (λ_*, α_*) is not present in the $\varepsilon = 0$ case. The calculation of this secondary bifurcation point allows us to estimate that equations (1.2) are bistable on the range

$$\lambda_*(\varepsilon) < \lambda < \lambda^*(\varepsilon). \tag{3.1}$$

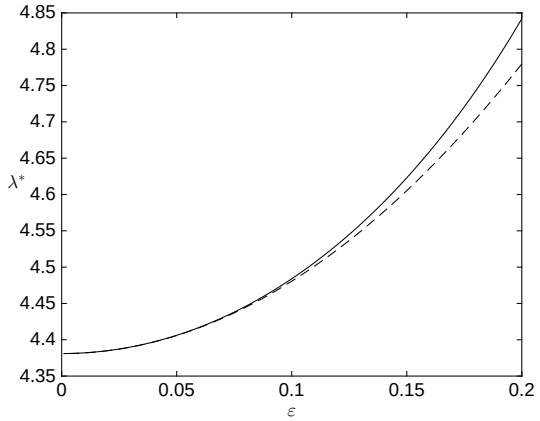

Fig. 4 A comparison of the asymptotic (dashed) and numerical (solid) predictions for the principal fold point of (2.7) in the case $m = 4$.

In addition, the system is predicted to lose bi-stability for $\varepsilon > \varepsilon_c$ where ε_c is defined implicitly by $\lambda_*(\varepsilon_c) = \lambda^*(\varepsilon_c)$. The calculation of $\lambda_*(\varepsilon)$ requires systematic use of switchback terms to obtain a well ordered expansion in the limit as $\varepsilon \to 0^+$.

In the vicinity of λ_* we stipulate that $u(0) = -1 + \varepsilon\alpha$ where $\alpha = \mathcal{O}(1)$ and obtain the parameterized bifurcation curve $(\lambda(\alpha;\varepsilon), \|u(\alpha;\varepsilon)\|_2)$ in the limit where $\varepsilon \to 0^+$. We assume that $\lambda(\varepsilon) \to 0$ as $\varepsilon \to 0^+$, so that in terms of some $\nu(\varepsilon) \ll 1$,

$$\lambda(\varepsilon) \sim \nu(\varepsilon)\lambda_0 + \cdots . \tag{3.2}$$

Since u_ε is even in x, we restrict (1.2) to $0 < x < 1$ and impose the symmetry conditions $u_x(0) = u_{xxx}(0) = 0$. In the outer region for $0 < x < 1$, we expand the solution as

$$u(x;\varepsilon) \sim u_0(x) + \nu(\varepsilon)u_1(x) + \cdots . \tag{3.3}$$

From (3.3) and (1.2), we obtain on $0 < x < 1$ that

$$u_{0xxxx} = 0\,, \quad 0 < x < 1\,; \qquad u_0(1) = u_{0x}(1) = 0\,, \tag{3.4a}$$

$$u_{1xxxx} = -\frac{\lambda_0}{(1+u_0)^2}\,, \quad 0 < x < 1\,; \qquad u_1(1) = u_{1x}(1) = 0\,. \tag{3.4b}$$

For (3.4a), we impose the point constraints $u_0(0) = -1$ and $u_{0x}(0) = 0$ in order to match to an inner solution below. This determines $u_0(x)$ as

$$u_0(x) = -1 + 3x^2 - 2x^3\,. \tag{3.5}$$

Since $u_{0xxx}(0) \neq 0$, u_0 does not satisfy the symmetry condition $u_{xxx}(0) = 0$. Thus, we need an inner layer near $x = 0$.

Upon substituting (3.5) into (3.4b), we obtain for $x \ll 1$ that

$$u_{1xxxx} = -\frac{\lambda_0}{(3x^2 - 2x^3)^2} = -\frac{\lambda_0}{9x^4}\left(1 - \frac{2x}{3}\right)^{-2} = -\frac{\lambda_0}{9x^4}\left(1 + \frac{4x}{3} + \frac{12x^2}{9} + \cdots\right).$$

Then, by integrating this limiting relation, we obtain the local behavior

$$u_1 \sim \frac{\lambda_0}{54}\log x - \frac{2\lambda_0}{27}x\log x + c_1 + b_1 x + \mathcal{O}(x^2\log x)\,, \text{ as } x \to 0\,, \tag{3.6}$$

in terms of constants c_1 and b_1 to be fixed. The determination of these constants then specifies the homogeneous component of the solution to u_1. From (3.3), (3.5), and (3.6), we obtain that

$$u(x;\varepsilon) \sim -1 + 3x^2 - 2x^3 + \nu\left(\frac{\lambda_0}{54}\log x - \frac{2\lambda_0}{27}x\log x + c_1 + b_1 x + \mathcal{O}(x^2\log x)\right) + \cdots, \quad \text{as} \quad x \to 0\,. \tag{3.7}$$

By introducing the inner variable $y = x/\gamma$, we have to leading order from (3.7) that $u \sim -1+3\gamma^2 y^2+\cdots$ as $x \to 0$. Since $u = -1+\mathcal{O}(\varepsilon)$ in the inner region, this motivates the scaling $\gamma = \varepsilon^{\frac{1}{2}}$ and the definition of local variables y and $w(y)$ where

$$y = \frac{x}{\varepsilon^{\frac{1}{2}}}\,, \qquad u = -1 + \varepsilon w(y)\,. \tag{3.8}$$

Next, we balance the cubic term $-2x^3$ in (3.7) with the $\mathcal{O}(\nu)$ term in (3.7) to get $\nu = \varepsilon^{\frac{3}{2}}$. Then, we substitute (3.8) and $\lambda(\varepsilon) \sim \varepsilon^{\frac{3}{2}}\lambda_0$ into (1.2), to obtain that $w(y)$ satisfies

$$-w_{yyyy} = \lambda_0 \varepsilon^{\frac{1}{2}} \left[\frac{1}{w^2} - \frac{1}{w^m}\right], \quad y > 0\,; \qquad w(0) = \alpha\,, \quad w_y(0) = w_{yyy}(0) = 0\,. \tag{3.9}$$

To determine the correct expansions for the inner and outer solutions, we write the local behavior of the outer expansion in (3.7) in terms of the inner variable $x = \varepsilon^{\frac{1}{2}} y$, with $\nu = \varepsilon^{\frac{3}{2}}$, to get

$$u(x;\varepsilon) = -1 + 3\varepsilon y^2 + \left(\varepsilon^{\frac{3}{2}}\log\varepsilon\right)\frac{\lambda_0}{108} + \varepsilon^{\frac{3}{2}}\left(-2y^3 + \frac{\lambda_0}{54}\log y + c_1\right) + \left(-\varepsilon^2\log\varepsilon\right)\frac{\lambda_0}{27}y \\ + \varepsilon^2\left[-\frac{2\lambda_0}{27}y\log y + b_1 y\right] + \mathcal{O}(\varepsilon^{\frac{5}{2}}\log\varepsilon)\,. \tag{3.10}$$

The terms of order $\mathcal{O}(\varepsilon^{\frac{3}{2}}\log\varepsilon)$ and order $\mathcal{O}(\varepsilon^2\log\varepsilon)$ must be accounted for with *switchback terms* in the outer expansion. In addition, the $\mathcal{O}(\varepsilon)$ term in (3.10), enables us to conclude that (3.9) should admit the expansion $w \sim w_0 + o(1)$, where w_0 satisfies

$$w_{0yyyy} = 0\,, \quad y > 0\,; \qquad w_0(0) = \alpha\,, \quad w_{0y}(0) = w_{0yyy}(0) = 0\,; \quad w_0 \sim 3y^2 \quad \text{as} \quad y \to \infty\,. \tag{3.11a}$$

This problem has the exact solution

$$w_0 = 3y^2 + \alpha\,. \tag{3.11b}$$

The constant term in (3.11b) then generates the unmatched term ε in the outer region, which can only be removed by introducing a second switchback term into the outer expansion. This suggests that $\lambda(\varepsilon)$, and the outer expansion for $u(x;\varepsilon)$, must have the form

$$u(x;\varepsilon) = u_0 + \varepsilon u_{\frac{1}{2}} + \left(\varepsilon^{\frac{3}{2}}\log\varepsilon\right) u_{\frac{3}{2}} + \varepsilon^{\frac{3}{2}} u_1 + \cdots\,, \qquad \lambda(\varepsilon) = \varepsilon^{\frac{3}{2}}\lambda_0 + \varepsilon^2\lambda_1 + \cdots\,. \tag{3.12}$$

Upon substituting (3.12) into (1.2), and collecting similar terms in ε, we obtain that $u_{\frac{1}{2}}$ satisfies

$$u_{\frac{1}{2}xxxx} = 0\,, \quad 0 < x < 1\,; \qquad u_{\frac{1}{2}}(0) = \alpha\,, \quad u_{\frac{1}{2}x}(0) = b_{\frac{1}{2}}\,, \quad u_{\frac{1}{2}}(1) = u_{\frac{1}{2}x}(1) = 0\,, \tag{3.13a}$$

where $b_{\frac{1}{2}}$ is a constant to be found. The condition $u_{\frac{1}{2}}(0) = \alpha$ accounts for the constant term in w_0. The solution is

$$u_{\frac{1}{2}}(x) = \alpha + b_{\frac{1}{2}}x + \left(-3 - 2b_{\frac{1}{2}}\right)x^2 + \left(b_{\frac{1}{2}} + 2\right)x^3\,. \tag{3.13b}$$

Similarly, $u_{\frac{3}{2}}(x)$ satisfies $u_{\frac{3}{2}xxxx} = 0$. To eliminate the $\mathcal{O}(\varepsilon^{\frac{3}{2}}\log\varepsilon)$ and $\mathcal{O}(\varepsilon^2\log\varepsilon)$ terms in (3.10), we let $u_{\frac{3}{2}}$ satisfy

$$u_{\frac{3}{2}xxxx} = 0\,, \quad 0 < x < 1\,; \qquad u_{\frac{3}{2}}(0) = -\frac{\lambda_0}{108}\,, \quad u_{\frac{3}{2}x}(0) = \frac{\lambda_0}{27}\,, \quad u_{\frac{3}{2}}(1) = u_{\frac{3}{2}x}(1) = 0\,. \tag{3.14a}$$

The solution for $u_{\frac{3}{2}}$ is

$$u_{\frac{3}{2}} = \lambda_0\left(-\frac{1}{108} + \frac{x}{27} - \frac{5x^2}{108} + \frac{x^3}{54}\right). \tag{3.14b}$$

We then substitute (3.5), (3.6), (3.13b), (3.14b), for u_0, u_1, $u_{\frac{1}{2}}$, and $u_{\frac{3}{2}}$ respectively, into the outer expansion (3.12), and write the resulting expression in terms of the inner variable $x = \varepsilon^{\frac{1}{2}} y$. This yields the following behavior for $u(x;\varepsilon)$ as $y \to \infty$:

$$\begin{aligned} u(x;\varepsilon) \sim -1 + \varepsilon\left(3y^2 + \alpha\right) + \varepsilon^{\frac{3}{2}}\left(-2y^3 + \frac{\lambda_0}{54}\log y + b_{\frac{1}{2}} y + c_1\right) \\ + \varepsilon^2\left(-(3 + 2b_{\frac{1}{2}})y^2 - \frac{2\lambda_0}{27} y\log y + b_1 y + \cdots\right). \end{aligned} \tag{3.15}$$

As $u = -1 + \varepsilon w(y)$ in the inner region, behavior (3.15) suggests the inner solution be expanded as

$$w = w_0 + \varepsilon^{\frac{1}{2}} w_1 + \varepsilon w_2 + \cdots. \tag{3.16}$$

Upon substituting (3.16) and (3.12) for $\lambda(\varepsilon)$ into (3.9), we obtain that w_0 satisfies (3.11), and that w_1, w_2 solve

$$w_{1yyyy} = -\frac{\lambda_0}{w_0^2} + \frac{\lambda_0}{w_0^m}, \quad y > 0; \qquad w_1(0) = w_{1y}(0) = w_{1yyy}(0) = 0, \tag{3.17a}$$

$$w_1 \sim -2y^3 + \frac{\lambda_0}{54}\log y + b_{\frac{1}{2}} y + c_1 + \cdots, \quad \text{as} \quad y \to \infty, \tag{3.17b}$$

$$w_{2yyyy} = \left[\frac{2\lambda_0}{w_0^3} - \frac{m\lambda_0}{w_0^{m+1}}\right] w_1 - \frac{\lambda_1}{w_0^2} + \frac{\lambda_1}{w_0^m}, \quad y > 0; \qquad w_2(0) = w_{2y}(0) = w_{2yyy}(0) = 0, \tag{3.18a}$$

$$w_2 \sim -(3 + 2b_{\frac{1}{2}})y^2 - \frac{2\lambda_0}{27} y\log y + b_1 y + \cdots, \quad \text{as} \quad y \to \infty. \tag{3.18b}$$

The solution to these problems determine λ_0, λ_1, $b_{\frac{1}{2}}$ and c_1 as is now shown. The value of λ_0 is first calculated by integrating (3.17a) over $(0,\infty)$ to give

$$\begin{aligned} 12 &= \lambda_0\left[\int_0^\infty \frac{\mathrm{d}y}{(\alpha + 3y^2)^2} - \int_0^\infty \frac{\mathrm{d}y}{(\alpha + 3y^2)^m}\right] = \lambda_0\sqrt{\frac{\alpha}{3}}\left[\frac{\pi}{4\alpha^2} + \frac{1}{\alpha^m}\int_0^{\frac{\pi}{2}} [\cos u]^{2(m-1)}\mathrm{d}u\right] \\ &= \frac{\lambda_0}{\sqrt{3}}\left[\frac{\pi}{4\alpha^{\frac{3}{2}}} - \frac{\sqrt{\pi}}{2\alpha^{m-\frac{1}{2}}}\frac{\Gamma(m-\frac{1}{2})}{\Gamma(m)}\right] \qquad \left[y = \sqrt{\alpha/3}\tan u\right]. \end{aligned}$$

which leads to the expression for λ_0

$$\lambda_0 = 12\sqrt{3}\left[\frac{\pi}{4\alpha^{\frac{3}{2}}} - \frac{\sqrt{\pi}}{2\alpha^{m-\frac{1}{2}}}\frac{\Gamma(m-\frac{1}{2})}{\Gamma(m)}\right]^{-1}, \qquad m > 2. \tag{3.19}$$

Here $\Gamma(z) = \int_0^\infty x^{z-1}e^{-x}\mathrm{d}x$. The correction term λ_1 is calculated from (3.18) by integrating (3.18a) over $0 < y < \infty$, and then applying $w_{2yyy} \to 0$ as $y \to \infty$, with $w_0 = \alpha + 3y^2$. This yields that

$$\lambda_1 = \frac{\lambda_0^2}{12}\int_0^\infty \left[\frac{2}{(\alpha + 3y^2)^3} - \frac{m}{(\alpha + 3y^2)^{m+1}}\right] w_1\,\mathrm{d}y. \tag{3.20}$$

This integral can be explicitly evaluated by solving for the exact solution $w_1(y)$ of (3.17). The first step is to calculate $w_{1yy}(0)$ and then formulate (3.17) as an initial value ODE problem for w_1. To do so, we multiply (3.17a) by w_{0y}, integrate over $0 < y < R$, then pass to the limit as $R \to \infty$, to obtain

$$\lim_{R\to\infty}\int_0^R w_{0y}w_{1yyyy}\,\mathrm{d}y = \lim_{R\to\infty}\left(w_{0y}w_{1yyy} - w_{0yy}w_{1yy}\right)\Big|_0^R + \lim_{R\to\infty}\int_0^R w_{1yy}w_{0yyy}\,\mathrm{d}y = 6w_{1yy}(0).$$

On the other hand,

$$-\lambda_0\lim_{R\to\infty}\int_0^R \frac{w_{0y}}{w_0^2} - \frac{w_{0y}}{w_0^m}\,\mathrm{d}y = \lambda_0\left(\frac{1}{w_0} - \frac{1}{(m-1)w_0^{m-1}}\right)\Big|_{y=0}^\infty = 6w_{1yy}(0). \tag{3.21}$$

Since $w_0(0) = \alpha$, this yields that

$$w_{1yy}(0) = \frac{\lambda_0[1-(m-1)\alpha^{m-2}]}{6(m-1)\alpha^{m-1}},$$

which together with the initial values $w_1(0) = w_{1y}(0) = w_{1yyy}(0) = 0$, allows the initial value problem (3.17) to be solved for w_1. A closed form of w_1 is available in terms of hyper geometric functions, though for general $m > 2$ it is quite cumbersome. For the particular value $m = 4$ for example, the solution is

$$\begin{aligned} w_1 = \frac{-\lambda_0}{864\alpha^{\frac{7}{2}}}\Bigg[& 3\sqrt{3}\, y \tan^{-1}\left(\sqrt{\frac{3}{\alpha}}y\right)\left[8\alpha^3 - \alpha + y^2(8\alpha^2-5)\right] \\ & + y^2(24\alpha^{\frac{5}{2}} - 15\alpha^{\frac{1}{2}}) - 8\alpha^{\frac{7}{2}}\log\left(1+\frac{3y^2}{\alpha}\right)\Bigg] \end{aligned} \tag{3.22}$$

The constants $b_{\frac{1}{2}}$ and c_1 are determined by applying the large argument expansion $\tan^{-1}(y) \sim \pi/2 - y^{-1} + (3y^3)^{-1}$ for $y \to \infty$ to (3.22) and comparing to (3.17b) to obtain for $m = 4$ that

$$c_1 = \frac{2\lambda_0}{81} - \frac{\lambda_0}{648\alpha^2} + \frac{\lambda_0 \log\frac{3}{\alpha}}{108}, \qquad b_{\frac{1}{2}} = \frac{2\alpha(1-8\alpha^2)}{8\alpha^2-5}. \tag{3.23}$$

The exact expression for w_1 in (3.22) allows λ_1 to be calculated by directly evaluating the integral (3.20). In this way, the formula for the case $m = 4$

$$\lambda_1 = 2\lambda_0^2\left[\frac{-595 + 32\alpha^2[235 - 210\log 2 + 48\alpha^2(3\log 2 - 4)]}{41472\alpha^3(8\alpha^2-5)}\right], \tag{3.24}$$

is found. For completeness, we remark that b_1 from (3.18b) is uniquely determined by first multiplying (3.18a) by w_0 followed by integrating over $(0, R)$ and evaluation of the limit $R \to \infty$. The details are omitted as the value of b_1 does not contribute to the location of the saddle node λ_* at this order.

Briefly summarizing the calculation so far, we have that in the vicinity of the saddle node bifurcation, the solution branch has parameterization

$$u(0) = -1 + \varepsilon\alpha, \qquad \lambda \sim \varepsilon^{\frac{3}{2}}\lambda_0(\alpha) + \varepsilon^2\lambda_1(\alpha) + \cdots,$$

The saddle-node bifurcation point (α_*, λ_*) is located by the condition $\lambda_\alpha(\alpha_*) = 0$ to be

$$\lambda_* = \lambda(\alpha_*) = \varepsilon^{\frac{3}{2}}\lambda_0(\alpha_{*0}) + \varepsilon^2\lambda_1(\alpha_{*0}) + \cdots$$

where the fold point is fixed by the condition $\lambda_\alpha(\alpha_*) = 0$ and α_{*0} is determined by

$$\lambda_{0\alpha}(\alpha_{*0}) = 0. \tag{3.25}$$

The values of α_{*0} and $\lambda_0(\alpha_{*0})$ are

$$\alpha_{*0} = \left[\frac{4(m-\frac{1}{2})}{3\sqrt{\pi}}\frac{\Gamma(m-\frac{1}{2})}{\Gamma(m)}\right]^{\frac{1}{m-2}}, \qquad \lambda_0(\alpha_{*0}) = \frac{48\sqrt{3}}{\pi}\frac{(m-\frac{1}{2})}{(m-2)}\alpha_{*0}^{\frac{3}{2}}. \tag{3.26}$$

The correction term $\lambda_1(\alpha_{*0})$ is more difficult to express in a closed form expression for general m as this requires solution of (3.17) followed by integration of (3.20). We therefore provide in Table 2, closed form expressions for these higher order corrections for selected values of m.

The preceding calculations are now summarized:

m	α_{*0}	$\lambda_0(\alpha_{*0})$	$\lambda_1(\alpha_{*0})$
3	$\frac{5}{4}$	$\frac{75\sqrt{15}}{\pi}$	$-\frac{5625}{8\pi^2}$
4	$\left(\frac{35}{24}\right)^{\frac{1}{2}}$	$\frac{7}{\pi}\left(\frac{105^3}{2}\right)^{\frac{1}{4}}$	$-\frac{26411}{64\pi^2}$
5	$\left(\frac{105}{64}\right)^{\frac{1}{3}}$	$\frac{27\sqrt{35}}{\pi}$	$-\frac{1143}{16\pi^2}\left(\frac{21^2}{5}\right)^{\frac{1}{3}}$

Table 2 Explicit expressions for terms of the asymptotic expansion of the saddle-node fold point (λ_*, α_*) for $m = 3, 4, 5$.

Principal Result 2 *In the vicinity of the secondary fold point λ_*, solutions of* (1.2) *admit the parameterization*

$$u(0) = -1 + \varepsilon\,\alpha, \qquad \lambda(\varepsilon) \sim \lambda_0(\alpha)\,\varepsilon^{\frac{3}{2}} + \lambda_1(\alpha)\,\varepsilon^2 + \cdots \tag{3.27a}$$

where λ_0 and λ_1 are given in (3.19) *and* (3.20) *respectively. In the limit as $\varepsilon \to 0$, a two term expansion for λ_* is given by*

$$\lambda_* \sim \lambda_0(\alpha_{*0})\varepsilon^{\frac{3}{2}} + \lambda_1(\alpha_{*0})\varepsilon^2 + \cdots \tag{3.27b}$$

where values of α_{*0}, $\lambda_0(\alpha_{*0})$, $\lambda_1(\alpha_{*0})$ are given by (3.26) *and* (3.20)*. For selected values of m, explicit expressions for these thresholds are given in Table 2. For example, in the case $m = 4$, we have that*

$$\begin{aligned}\lambda_* &\sim \frac{7}{\pi}\left(\frac{105^3}{2}\right)^{\frac{1}{4}}\varepsilon^{\frac{3}{2}} - \frac{26411}{64\pi^2}\varepsilon^2 + \cdots \\ &\sim 61.4586\,\varepsilon^{\frac{3}{2}} - 41.8124\,\varepsilon^2 + \cdots .\end{aligned} \tag{3.27c}$$

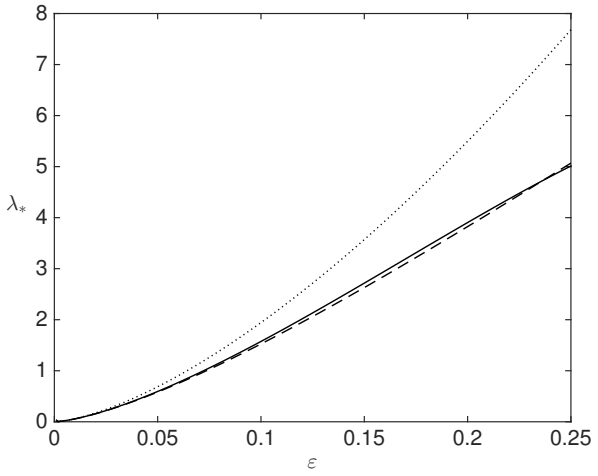

Fig. 5 Numerical validation of Principal Result 2. Comparison of λ_* from one term asymptotic (dotted), two term asymptotic (dashed) and numerical (solid) approximations.

3.1 Prediction of the bistable region.

The analysis of the previous sections has focussed on accurately determining two saddle-node bifurcation points, $\lambda^*(\varepsilon)$ and $\lambda_*(\varepsilon)$. When combined, these two values predict that equations (1.2) are bistable on the range

$$\lambda_*(\varepsilon) < \lambda < \lambda^*(\varepsilon). \tag{3.28}$$

In terms of the expressions derived in Principal Results 1 and 2 for $\lambda^*(\varepsilon)$ and $\lambda_*(\varepsilon)$ respectively, the bistable region for the case $m = 4$ is predicted to be

$$61.4586\,\varepsilon^{\frac{3}{2}} - 41.8124\,\varepsilon^2 < \lambda < 4.3809 + 9.9713\,\varepsilon^2. \tag{3.29}$$

A heuristic prediction of ε_c, the threshold for bi-stability can be obtained by solving the equation $\lambda_*(\varepsilon_c) = \lambda^*(\varepsilon_c)$ for each of the above cases. These predictions are encapsulated in the following Principal Result

Principal Result 3 *The asymptotic formulation* (3.29) *for the fold points* $\lambda^*(\varepsilon)$ *and* $\lambda_*(\varepsilon)$ *associated with the equilibrium problems* (1.2) *coalesce at* ε_c *where asymptotic and numerical estimates of* ε_c *are given by*

$$\begin{aligned}
m = 3: &\quad \varepsilon_c \sim 0.2102 \quad (Asymptotic), &&\quad \varepsilon_c \sim 0.2319 \quad (Numerical);\\
m = 4: &\quad \varepsilon_c \sim 0.2468 \quad (Asymptotic), &&\quad \varepsilon_c \sim 0.2727 \quad (Numerical);\\
m = 5: &\quad \varepsilon_c \sim 0.2646 \quad (Asymptotic), &&\quad \varepsilon_c \sim 0.3039 \quad (Numerical).
\end{aligned}$$

Consequently, equation (1.2) *is predicted to be bistable on the range* $0 < \varepsilon < \varepsilon_c$ *and to admit a unique solution for each* $\lambda \geq 0$ *whenever* $\varepsilon \geq \varepsilon_c$.

In Principal Result 3, the cubic fold point (α_c, λ_c), corresponding to the threshold of bistability in (1.2), is located by numerical solution of the system

$$\begin{bmatrix} \lambda_\alpha(\alpha_c, \varepsilon_c) \\ \lambda_{\alpha\alpha}(\alpha_c, \varepsilon_c) \end{bmatrix} = \begin{bmatrix} 0 \\ 0 \end{bmatrix}. \tag{3.30}$$

We remark that in Principal Result 3, agreement between the asymptotic and numerical results is quite close ($\approx 10\%$), especially given that is is derived from the heuristic condition that the bistable range (3.29) shrinks to a point.

4 Conclusion

In this paper we have studied equilibrium states of the regularized model (1.1) which accounts for repulsive forces which become important when the gap spacing is very small. The problem of stiction is explained in this setting by the presence of bistability in this system when $\varepsilon < \varepsilon_c$. The main practical contribution of this work is a framework for accurately estimating the conditions for bistability in the system. Namely, for $\varepsilon < \varepsilon_c$ the system is bistable on the parameter range $\lambda_* < \lambda < \lambda^*$ and we have established accurate estimates of the three key thresholds ε_c, λ_* and λ^* for $m > 2$.

There are many avenues of future investigation that arise from this work. It is highly desirable to rigorously verify the bistable nature of (1.1) and establish the existence of solutions for all $m > 2$ and in higher dimensional settings. A study of stiction in the more practically relevant two-dimensional setting would reveal additional factors that contribute to stiction such as contact line energies and dependence on device geometry.

There are significant challenges which can be anticipated to arise in such an extension. First, the methods used (Sec. 3) to calculate λ_* require exact expressions for the singular limiting solution, which is essentially the Green's function for the bi-Laplacian. Such expressions are not available in higher dimensional settings except in the most simple situations. Progress can be made by employing a combination of exact knowledge of the singularity structure with numerical calculation of quantities associated with the associated regular part (cf. [30]). Second, in spatial dimension $d = 2$ the singularity structure associated with the Green's function is $r^2 \log r$. This can be expected to generate a more complex asymptotic expansion for the fold point λ_*, featuring an infinite logarithmic series as $\varepsilon \to 0$. Such series are common in singular perturbation problems in two dimensions and unfortunately converge very slowly. An interesting problem would be to formulate a hybrid asymptotic numerical method (cf. [34, 35]) to accelerate this convergence and obtain accurate estimates of the bistability range of MEMS devices with a wide variety of geometries.

Acknowledgements AEL gratefully acknowledges many useful discussions with J. Lega and K. B. Glasner and support from the National Science Foundation under grant DMS-1516753.

References

1. W Merlijn van Spengen, Robert Puers, Ingrid De Wolf *A physical model to predict stiction in MEMS*, J. Micromech. Microeng. (2002) **12** 702
2. N. Tas, T Sonnenberg, H. Jansen, R. Legtenberg and M. Elwenspoek, *Stiction in surface micromachining*, J. Micromech. Microeng **6** (1996) pp. 385–397.
3. Y.-P. Zhao, L.S. Wang and T. X. Yu, *Mechanics of adhesion in MEMS*, J. Adhesion Sci. Technol., Vol. 17, No. 4, pp. 519–546. (2003).
4. Y. Guo, Z. Pan, M. J. Ward, *Touchdown and Pull-In Voltage Behaviour of a MEMS Device with Varying Dielectric Properties*, SIAM J. Appl. Math., **66**, No. 1, (2005), pp. 309–338.
5. F. H. Lin, Y. Yang, *Nonlinear Non-Local Elliptic Equation Modeling Electrostatic Actuation*, Proc. Roy. Soc. A, **463**. (2007), pp. 1323–1337.
6. J. A. Pelesko, *Mathematical modeling of electrostatic MEMS with tailored dielectric properties*, SIAM Journal on Applied Mathematics, v. 62, pp. 888–908, 2002.
7. J. A. Pelesko, D. H. Bernstein, *Modeling MEMS and NEMS*, Chapman Hall and CRC Press, (2002).
8. A. E. Lindsay, J. Lega, K.B. Glasner, *Regularized Model of Post-Touchdown Configurations in Electrostatic MEMS: Equilibrium Analysis* Physica D: Nonlinear Phenomena (2014) Vol. 280-281, pp. 95–108.
9. Jian-Gang Guo, Ya-Pu Zhao, *Influence of van der Waals and Casimir Forces on Electrostatic Torsional Actuators*, Journal of Microelectromechanical systems, Vol. 13, No. 6, 2004, pp. 1027–1035.
10. F. Michael Serry, Dirk Walliser, G. Jordan Maclay, *The role of the casimir effect in the static deflection and stiction of membrane strips in microelectromechanical systems (MEMS)*, Journal of Applied Physics, Vol. 84, No. 8, (1998).
11. Romesh C. Batra, Maurizio Porfiri, and Davide Spinello, *Effects of van der Waals Force and Thermal Stresses on Pull-in Instability of Clamped Rectangular Microplates*, Sensors 2008, **8**, pp. 1048–1069.
12. DelRio, Frank W., de Boer, Maarten P., Knapp, James A., David Reedy, E., Clews, Peggy J., Dunn, Martin L., *The role of van der Waals forces in adhesion of micromachined surfaces*, Nat Mater, **4**, 2005, pp. 629–634.
13. Y.-P. Zhao, *Stiction and anti-stiction in MEMS and NEMS*, Acta Mechanica Sinica, Vol. 19, No. 1 (2003).
14. A. J. Bernoff and T. P. Witelski, *Stability and dynamics of self-similarity in evolution equations*, Journal of Engineering Mathematics, vol. 66 no. 1-3 (2010), pp. 11–31, ISSN 1573–2703.
15. A. J. Bernoff, A. L. Bertozzi and T. P. Witelski, *Axisymmetric surface diffusion: Dynamics and stability of self-similar pinch-off*, J. Stat. Phys. (1998) 93, 725–776.
16. A. L. Bertozzi, G. Grün and T. P. Witelski, *Dewetting films: bifurcations and concentrations*, Nonlinearity **14** (2001) 1569–1592.
17. A. J. Bernoff and T. P. Witelski, *Stability of self-similar solutions for Van der Waals driven thin film rupture*, Physics of Fluids, Vol. 11 No. 9 (1999).
18. P. Esposito, N. Ghoussoub, Y. Guo, *Mathematical Analysis of Partial Differential Equations Modeling Electrostatic MEMS*, Courant Lecture Notes, (2010).
19. A. E. Lindsay, M. J. Ward, *Asymptotics of some nonlinear eigenvalue problems for a MEMS capacitor: Part II: Singular Asymptotics*, Euro. Jnl of Applied Mathematics (2011), vol. 22, pp. 83-123.
20. Slava Krylov, Bojan R. Ilic, Stella Lulinsky, *Bistability of curved microbeams actuated by fringing electrostatic fields*, Nonlinear Dyn (2011) 66: pp. 403–426.

21. Slava Krylov, Bojan R Ilic, David Schreiber, Shimon Seretensky, and Harold Craighead, *The pull-in behavior of electrostatically actuated bistable microstructures*, J. Micromech. Microeng. 18 (2008) 055026 (20pp)
22. Jin Qiu, Jeffrey H. Lang, and Alexander H. Slocum, *A Curved-Beam Bistable Mechanism*, Journal of Microelectromechanical Systems, Vol. 13, No.2, (2004), pp. 137–146.
23. A. E. Lindsay, J. Lega, K. B. Glasner, *Regularized Model of Post-Touchdown Configurations in Electrostatic MEMS: Interface Dynamics* (2015), IMA Journal of Applied Math, doi: 10.1093/imamat/hxv011
24. B. Lai, *On the Partial Differential Equations of Electrostatic MEMS with Effects of Casimir Force*, Annales Henri Poincaré, Vol. 16, No. 1 (2015) pp. 239–253.
25. R. Zhang, L. Cai, *On the semi linear equations of electrostatic NEMS devices*, Z. Angew. Math. Phys. 65 (2014) pp. 1207–1222.
26. P. Lagerstrom, Matched Asymptotic Expansions: Ideas and Techniques, Applied Mathematical Sciences, **76**, SpringerVerlag, New York, (1988).
27. N. Popovic, P. Szymolyan, A Geometric Analysis of the Lagerstrom Model Problem, J. Differential Equations, **199**, No. 2, (2004), pp. 290–325.
28. N. Popovic, P. Szymolyan, Rigorous Asymptotic Expansions for Lagerstrom?s Model Equation - A Geometric Approach, Nonlinear Anal., **59**, No. 4, (2004), pp. 531–565.
29. P. Lagerstrom, D. Reinelt, Note on Logarithmic Switchback Terms in Regular and Singular Perturbation Problems, SIAM J. Appl. Math., **44**, No. 3, (1984), pp. 451–462.
30. M.C. Kropinski, A.E. Lindsay, M.J. Ward, *Asymptotic Analysis of Localized Solutions to Some Linear and Nonlinear Biharmonic Eigenvalue Problems*, Studies in Appl. Math., **126**(4), (2011), pp. 347–408.
31. A. E. Lindsay, M. J. Ward, *Asymptotics of Some Nonlinear Eigenvalue Problems for a MEMS Capacitor: Part I: Fold Point Asymptotics*, Methods Appl. Anal., **15**, No. 3, (2008), pp. 297–325.
32. N. D. Brubaker and J. A. Pelesko, *Non-Linear Effects on Canonical MEMS Models*, European J. Appl. Math, No. 5, Vol. 22, (2011), pp. 455-470.
33. E. Van De Velde, M. J. Ward, *Criticality in Reactors Under Domain or External Temperature Perturbation*, Proc. R. Soc. Lond. A, No. 1891, (1991), pp. 341-367.
34. S. Hormozi, M. J. Ward, *A hybrid asymptotic-numerical method for calculating drag coefficients in 2-D low Reynolds number flows*, Journal of Engineering Mathematics, 2014.
35. M. C. Kropinski, M. J. Ward, J. B. Keller, *A Hybrid Asymptotic-Numerical Method for Calculating Low Reynolds Number Flows Past Symmetric Cylindrical Bodies*, SIAM J. Appl. Math., Vol. 55, (1995) pp. 1484–1510.